First Laboratory Demonstration of Anti-Halo Apodization: A Coronagraph "Afterburner"

Johanan L. Codona
Steward Observatory, University of Arizona

ABSTRACT

A prototype of the AntiHalo Apodization (AHA) system has been implemented and initially demonstrated in the lab. This system uses the diffraction-limited core starlight, normally discarded by the focal plane stop in a coronagraph, to explicitly construct a negative copy of the halo directly in the focal plane. When coherently combined with the coronagraphic halo in the detector plane, the resultant halo is expected to be up to 100× fainter. The total system design includes measuring the complex sum of the halo and the antihalo with an interferometric focal plane wavefront sensor (FPWFS), which is also implemented in the lab. In this progress report, we show initial results from creating the antihalo with a 2-DM Michelson spatial light modulator, and the first modest halo suppression achieved by using an intensity-minimizing search algorithm in the 2-dimensional AHA actuator displacement space. The resulting attenuation of a factor of 6 to 8×, points the way to the expected 2 decades of attenuation when the system is fully functional.

INTRODUCTION

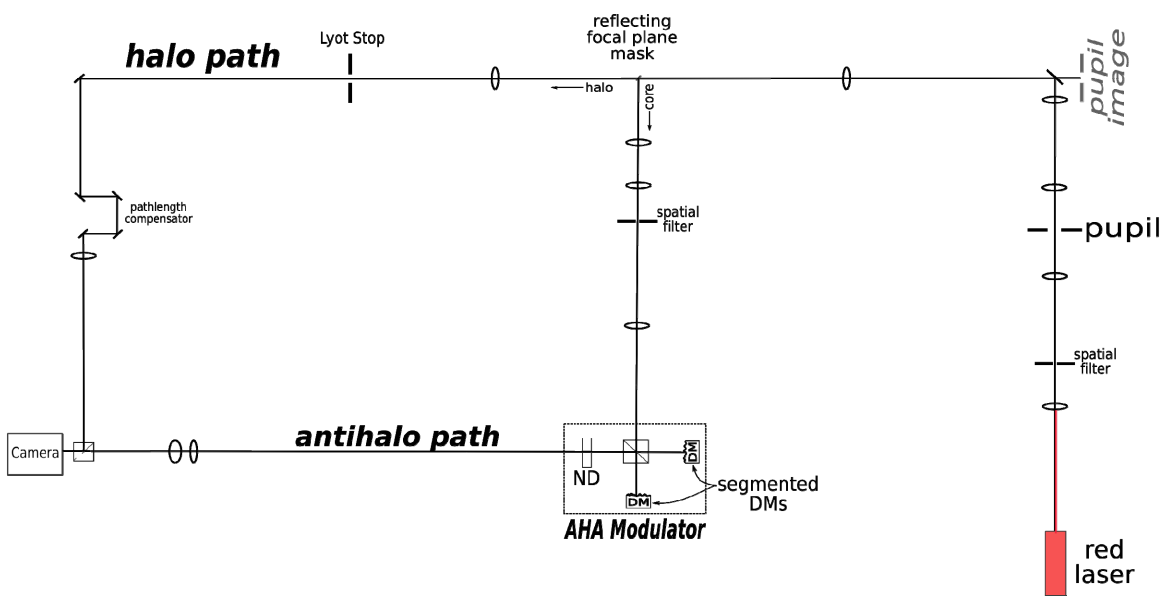

Figure 1: *Schematic of the Antihalo Testbed, showing only those paths and components used in this initial test.*

As this conference has clearly shown, great advances are being made in the design of stellar coronagraphs. To be able to see terrestrial exoplanets, the stellar halo needs to be suppressed on the order of ten decades below the diffraction peak of the star. This requirement is extremely difficult to meet, and indeed many promising techniques are falling 3 or 4 decades short of the mark. These problems are typically due to slight imperfections in manufacturing, or even very slight transmission variations, such as dust on the optical surfaces, which will cause halo light at levels much brighter than desired.

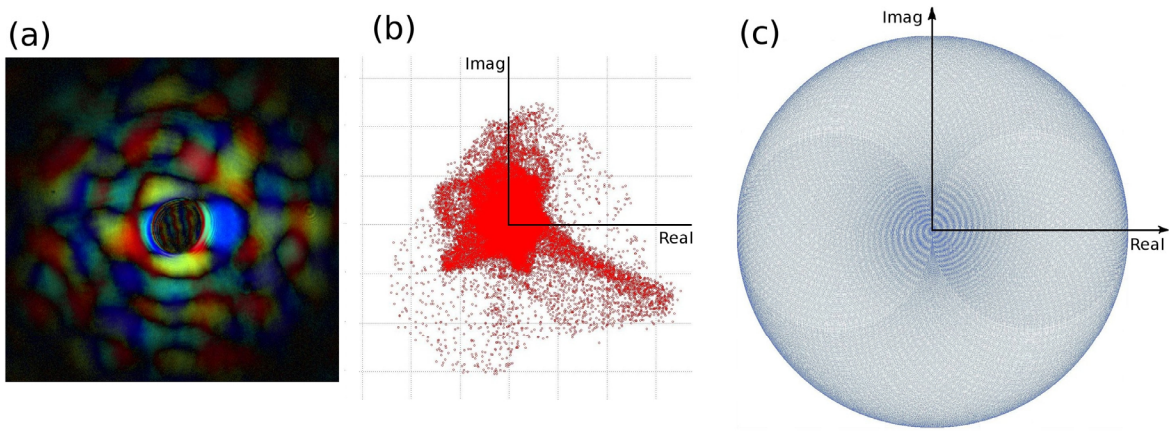

Figure 2: *Complex halo and addressable antihalo. (a) The complex halo can be measured using the FPWFS. This figure shows intensity as usual, but encodes phase as color. (b) The halo plotted as points in the complex plane. (c) A single wrap subset of addressable points in the complex plane using the MEMS DM and the high-resolution electronics.*

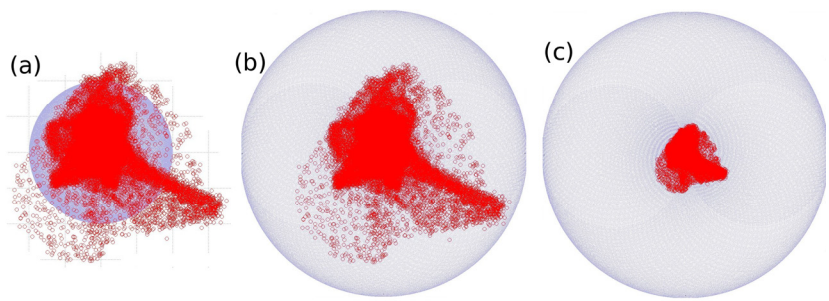

Figure 3: *Effect of AHA modulator illumination on addressable complex antihalo values. (a) AHA path too faint: can't reach or suppress all points in the halo. (b) AHA modulator illumination well matched to the halo. (c) AHA modulator illumination too bright: will work, but density of addressable points is lower limiting the maximum suppression.*

Since the scattered light halo is coherent with itself at various points in the focal plane, it is possible to mitigate the unwanted scattered light by measuring or estimating its phase and amplitude (i.e., its complex amplitude), and adjusting an upstream deformable mirror (DM) to intentionally create a speckle with the same amplitude but opposite sign, canceling the halo at that point. An iterative scheme can do this over a region, up to 180° around the star, and out to the control radius of the DM. The difficulty comes from the required level of control of the DM. To control a halo structure 10 decades below the star in visible light using a 1024-actuator DM would require each actuator to be controllable to about 10 pm.

The Anti-Halo Apodization (AHA) method is an active halo suppression technique that is intended to further suppress the residual halo achieved by a coronagraph (Codona and Angel, 2004). It accomplishes this by explicitly constructing a negative approximation of the residual halo directly in the focal plane and adding it to the halo, approximately canceling it out. To do this, the constructed antihalo must be temporally coherent with the residual coronagraph halo. In most coronagraph designs, the core starlight is blocked by a focal plane mask of some description, and is absorbed or otherwise prevented from further propagation though the coronagraph. We make the simple modification of diverting this discarded starlight and using it to create our temporally coherent antihalo. This method is similar to that originally proposed by Angel (2003) to build an interferometric focal plane wavefront sensor (FPWFS). Our system simultaneously implements both methods by splitting the core starlight: one part to build the antihalo, and the other part to interferometrically probe the sum of halo and antihalo.

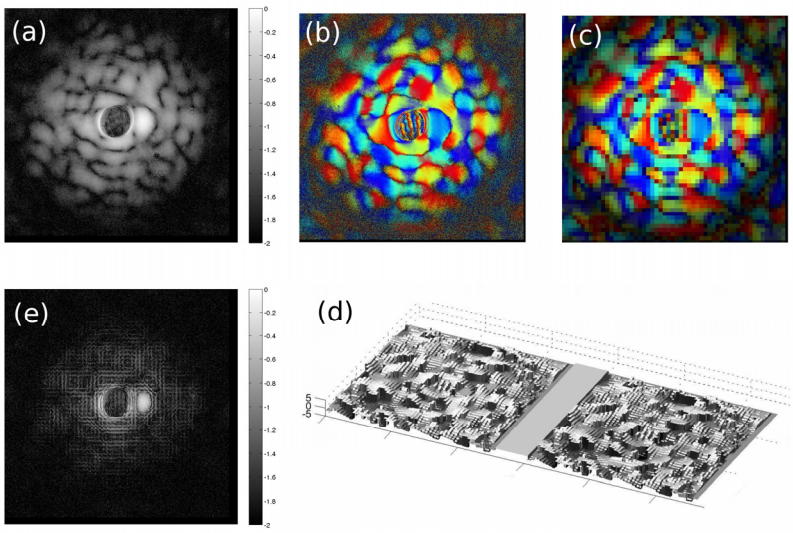

Figure 4: *Conceptual flow of the AHA method. (a) A measured intensity image of a speckled halo (high-gamma stretch). (b) The complex halo as measured with the FPWFS. (c) Pixelized version implemented on the AHA modulator. (d) The computed displacements for the two DMs in the AHA Michelson to create (c). (e) The intensity resulting from the difference between (b) and (c). Note the bright speckle at the 3:00 position that was too bright to be reached by the addressable complex values with the AHA modulator illumination. Increasing the modulator illumination would enable this speckle to also be suppressed.*

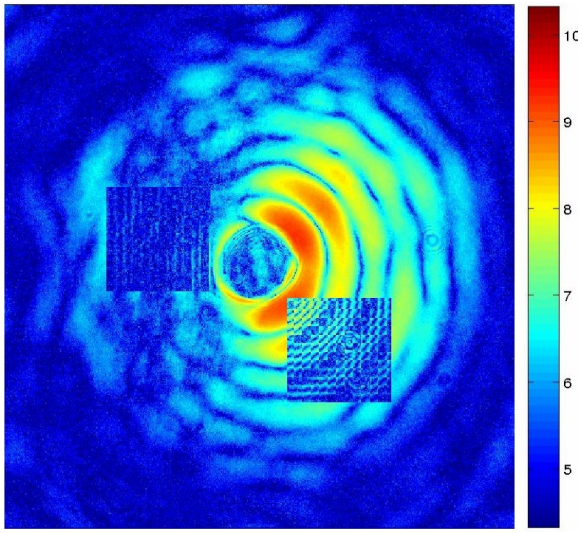

Figure 5: *With small DMs (say 12×12 actuators), only a small region of the focal plane may be suppressed. However, there are no restrictions on where it may be placed.*

The beauty of the AHA method is that the amount of starlight used to create the antihalo is controlled by some gross method, such as an ND filter, rather than by the incredibly fine control of a pupil DM. The additional suppression potentially achievable using AHA is inversely proportional to the density of addressable points in the antihalo complex plane. As discussed in Codona & Angel 2004, the suppression achievable by controlling the phase of each of the elements in the AHA SLM to 0.1 radians is about two decades. Using a MEMS DM with adequately high-resolution electronics should enable suppression at even higher levels, up to three decades. This assumes that the AHA "pixels" (the AHA spatial light modulator (SLM) actuators) are small compared with λ/D so that the uncontrolled shape of the antihalo over the actuator is not important. Since this technique works in conjunction with other coronagraph designs as an "afterburner" to get even more contrast out of the system, the addition of a relatively low-precision AHA system would significantly ease the accuracy and control requirements on the coronagraph and pupil DM, to levels such as a quarter of a nanometer, which is more robustly available.

At the time of this conference, we have just built the first laboratory implementation of an AHA modulator. As a first test, we used a single actuator search algorithm to perform a search in phase and amplitude to suppress the halo+antihalo. This process was repeated for a number of pixels over a rectangular test region. This first test, even with its algorithmic simplifications and the fact that it was search-based rather than using the FPWFS, successfully demonstrates and validates the AHA principle.

Lab Setup

In addition to the AHA technique, the UA Antihalo Testbed is intended to demonstrate and explore the use of the interferometric FPWFS, and a number of other adaptive halo suppression techniques and algorithms. Since the first test use of the AHA modulator did not involve these other components and subsystems, we will not describe them here. The relevant components are shown in Figure 1. Our light source was a simple red laser diode, which

was spatially filtered and collimated onto a pupil. This pupil is reimaged to another plane (to facilitate the use of a pupil DM not used here), and then imaged into the first focal plane of the coronagraph. Here there is a reflecting spot deposited on a glass substrate, with a 1:1.414 axial ratio, mounted on a 45° plane so that it appears to be a simple circular top hat mask when seen along the axis of the incoming light. The mask size used is comparable with the diameter of the first null in the Airy pattern. The light missing the mask is processed as usual for a normal Lyot coronagraph, being reimaged into a pupil plane where there is a Lyot stop, and finally being reimaged into a focal plane on the camera sensor. To enable the halo to remain in temporal coherence with the antihalo, the extra path length introduced by the AHA modulator must be added to the otherwise rectangular path. The diverted core light is spatially filtered and collimated onto the two segmented MEMS DMs of the AHA modulator. The light is split equally between the two mirrors with a 50/50 beam-splitter cube, which then remixes the reflected light with the phase modulation applied by moving the DM actuators. In the process, half the light entering the modulator is lost, but since it only needs to be a tiny fraction of the core starlight for an already faint halo, the loss is unimportant. Overall, the amplitude of the AHA modulator light is adjusted with a neutral density (ND) filter to have an input amplitude that is greater than that of any halo amplitude over the region to be suppressed. Finally, the newly imprinted antihalo is mixed with the residual halo from the coronagraph in another beam-splitting cube and is detected by the camera.

The AHA modulator is a fully complex spatial light modulator (SLM) built using a Michelson interferometer with a MEMS DM on each arm. The incoming light, having been spatially filtered and spread out over what will become the suppressed region of the halo, is intended to have no significant phase or intensity features. (In the full system, if it did, the FPWFS would automatically measure and compensate for them.) For optimal contrast and chromatic performance, the two arms of the modulator should be as close as possible to the same length, which should be similarly close to the path length of the halo path. The bandwidth and structure of the laser diode source used here is sufficiently broad to warrant careful alignment for best performance. However, for this first quick test, the only alignment done was to get high-contrast fringes in the AHA Michelson, and acceptable modulation between the antihalo and halo paths. Later, more careful adjustment will be necessary to achieve the best possible halo suppression. By examining the image of the illuminated AHA DMs from the final focal plane camera, the DMs were adjusted relative to each other so that their actuator images overlapped each other to within a small fraction of an actuator (roughly 30 microns on an actuator pitch of 0.3 mm).

By moving the DM actuators, the path length along each arm is altered, causing the phase shift along each arm to become $\phi arm=4\pi zarm/\lambda$, where zarm is the path length to an actuator along one of the arms. After remixing the light in the beam splitter cube, the resulting complex amplitude applied to the featureless field derived from the diffraction core is proportional to

$$\exp\{i\phi_1(x,y)\} + \exp\{i\phi_2(x,y)\}.$$

This is sufficient to give the antihalo any complex value inside a circle of radius controlled by the ND filter (Figure 2c). The DM control electronics start with a digital-to-analog converter (DAC), which generates an equally spaced set of voltages, which are applied to the actuators. The actuators, in turn, feel a force that is proportional to the square of the applied voltage opposing a linear restoring force, and hence the displacement is roughly proportional to the square of the voltage. The resulting, non-uniform set of surface displacements determines the spacing of the AHA complex modulator points. Since the goal is to create an antihalo replica of the halo, which is to be subtracted from it, controllability residual field error is determined by the distance between the nearest addressable antihalo point and the actual halo value. This means that the mean error field is proportional to the distance between the antihalo complex field points, and the resulting intensity is inversely proportional to the density of addressable points in the complex plane. To achieve maximum control of the actuators, we worked with the company *IrisAO, Inc.*, to adapt their high-resolution *Smart Driver* electronics to drive 128 of the 140 actuators in two *Boston Micromachines* DMs. The DM electronics, like the rest of the experimental control and data acquisition systems were controlled from a Linux system.

To understand the role of the ND filter in adjusting the resolution of the AHA modulator, imagine measuring the complex halo over the region to be suppressed, and plotting all of the field points in the complex plane (Figure 2). The circular set of addressable antihalo field points has a maximum amplitude which is determined by the amount of light passed through the AHA modulator, and is attenuated further by the ND filter. As can be seen in Figure 3a, if the set of antihalo points is smaller than the set of halo points (i.e., the AHA light is too dim), it will not be possible to fully suppress the brightest portions of the halo. If the AHA light is too bright (Figure 3c), all points in the halo will be able to be suppressed, but since the mean distance between the addressable points is larger, the maximum suppression will be less. The optimum setting is when the antihalo set is larger than the set of halo field points to be suppressed, but not too much larger (Figure 3b). This is well defined when the halo is stable, but if it is fluctuating, the best setting will be to adjust the maximum antihalo to be larger than the largest expected halo values.

The loss of suppression caused by having too much light passing through the AHA modulator is not serious in practice, since the finite actuator size limits our ability to fit the shape of the antihalo to the halo. The smallest halo structure scales are on the order of the diffraction scale, λ/D. Over this scale, full amplitude swings and sign reversals are common, and must be reproduced in detail for full suppression. We use segmented DMs to avoid problems with the influence functions near points where the halo field changes sign. However, if the segmented actuators are flat, the best halo-antihalo difference will have a triangular error with a magnitude proportional to the angular gradient of the field over the scale of the actuator. This means that there is a halo-fitting error intensity that is proportional to the square of the ratio of AHA modulator actuator size to the diffraction scale. Using a zoom lens arrangement allows this to be modified, but it also has the effect of shrinking the overall field that can be suppressed. Larger DMs will ease this problem in the future. For now, we nominally use a magnification of about 3 to 4 actuators per λ/D. This should ultimately allow for greater than 2 to 3 decades of suppression, which is still much greater than the electronics will allow.

The operational concept is illustrated in Figure 4. The halo used in this figure was actually measured using the focal plane interferometer, but the AHA portion was simulated. In Figure (4a), we have the speckled halo of a star imaged through a weak phase screen. The Strehl ratio is still high enough to retain a substantial diffraction-limited core, which was reflected for use as the reference beam in the FPWFS, and available for use in creating the AHA antihalo. There is a bright speckle at the 3-o'clock position that we will intentionally miss with the AHA modulator illumination, just to show the effect. Figure (4b) shows the complex halo as measured with the FPWFS, and (4c) shows the pixelized version of the halo that can be created using the AHA modulator for some illumination strength. This is accomplished by adjusting the two DM surfaces to appropriate values, shown in Figure (4d) for a hypothetical huge DM. The two surfaces are very similar when the desired antihalo amplitude is much fainter than the light illuminating the modulator, and differ more where the antihalo is brightest. Careful examination of the two surfaces near the positions of the brightest speckles shows this effect. Finally, Figure (4e) shows the result of the complex sum of the halo and antihalo, which takes place in the final beam splitter. Since the light directly entering the camera is *halo-antihalo*, while the light exiting the beam splitter in the other direction is *antihalo-halo*, capturing both outputs and summing the detected photons means that no light need be lost in the mixing stage. Figure 5 illustrates the current situation, where we have only a relatively small format DM with which to build the AHA modulator. In that case, the suppressed region is small, but may be placed anywhere within the focal plane.

FIRST RESULTS

The first test of AHA was intended to demonstrate the mechanics of the halo interfering with a manufactured antihalo—with at least some attenuation. For this purpose, it was not necessary to use the FPWFS to measure the complex sum of the halo and antihalo. Instead, we used a simple search algorithm in the two-dimensional actuator displacement space to find the best suppression for a single actuator. Although this algorithm is fully independent of what the other actuators are doing, and is completely parallelizable, the first test was performed one actuator pair at a time. The result is shown in Figure 6. The first image (Fig. 6a) is an intensity image of the halo in the region to be suppressed. The second image (Fig. 6b) is the halo mixed with the antihalo, but set to

default initial positions. Finally, after sequentially running the AHA search algorithm on a single actuator pair (Fig. 6c) and a rectangular subset of the modulator actuators (Fig. 6d), the halo is suppressed. The maximum suppression shown here was only a factor of 6 to 8. But given that this was simply an initial demonstration, and the system was not optimally aligned for maximum visibility, nor was the search algorithm designed to find the best null near the white light null, this level of attenuation was reasonable. Analysis of these results suggests that the full expected suppression should be achieved when the system is properly adjusted.

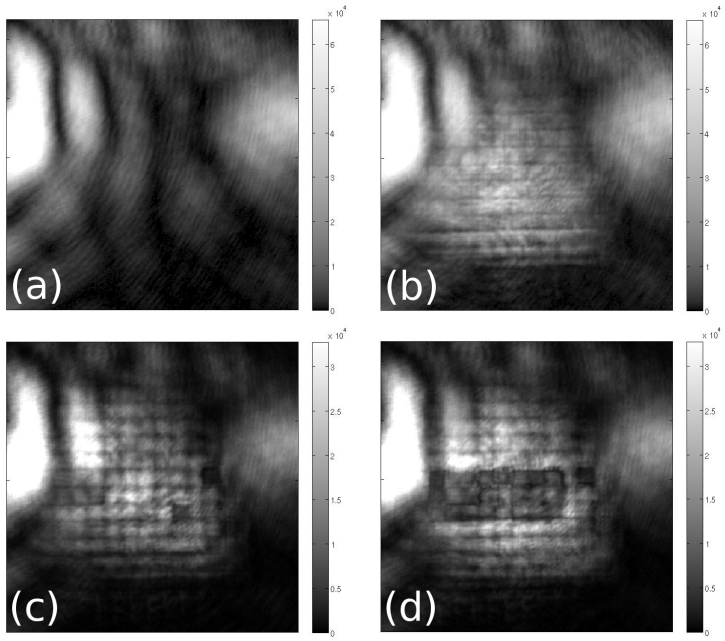

Figure 6: *Results of first AHA test. Bright ring on the left is the second Airy ring. (a) Initial halo. (b) Halo plus unset antihalo. (c) AHA effect after searching for a solution to a single AHA "pixel" value. (d) Repeated application of the single AHA "pixel" algorithm over a rectangular subset of the AHA region of the focal plane.*

SUMMARY

The AHA system is now working, and initial tests have validated the operational concept. Work continues in the lab to get the maximum suppression from the AHA modulator, along with simultaneous operation of the FPWFS, which will enable a closed-loop servo by measuring the complex field resulting from the coherent combination of the halo and the antihalo. We expect that when used with any coronagraph design where the discarded stellar core can be coherently preserved as a source for constructing the antihalo, the AHA method should permit 2 to 3 decades of improved halo suppression over that achieved by the coronagraph alone.

ACKNOWLEDGMENTS

Thanks to graduate student Peng Su for assistance in the lab. This work was supported by NASA grant Grant# NNG05GD28G.

REFERENCES

Angel, Roger, "Imaging Exoplanets from the Ground", in *Scientific Frontiers in Research on Extrasolar Planets*, eds. S. Seager and D. Deming, ASP Conf. Ser., 294, 543–556, Washington D.C. 2003.

Codona, J. L. and Roger Angel, "Imaging extrasolar planets by stellar halo suppression in separately-corrected color bands", ApJ **605**, L117–L120, 2004.